DISCHARGE OF CF_3I IN A COLD SIMULATED AIRCRAFT ENGINE NACELLE

Jiann C. Yang[§], Samuel L. Manzello, and Marc R. Nyden
Building and Fire Research Laboratory
National Institute of Standards and Technology
100 Bureau Drive, Gaithersburg, Maryland 20899, U.S.A.

Michael D. Connaghan
U.S. Army CECOM Research, Development, and Engineering Center
Fort Belvoir, Virginia 22060, U.S.A.

[§]Telephone: (301) 975-6662
Fax: (301) 975-4052
E-mail: jiann.yang@nist.gov, samuel.manzello@nist.gov, marc.nyden@nist.gov,
Michael_D_Connaghan@belvoir.army.mil

INTRODUCTION

An aircraft engine nacelle refers to the region between the engine body and its casing. Fuel and hydraulic lines, pumps, and lubrication systems are located within the nacelle. Air is vented through the nacelle to prevent any build-up of combustible vapors, and underside drain holes are used to mitigate potential pooling of flammable fluids as a result of a leak. Once a fire is detected in the nacelle, the pilot will first level the aircraft before arming and discharging the fire suppressant. Depending on the configuration of the aircraft, the fire suppression bottle is mounted either adjacent to the engine nacelle or at a location several meters away from the nacelle, and the agent is transported through piping to the fire zone.

Current aircraft fire suppression bottles for engine nacelle fire protection are normally filled with liquid CF_3Br (halon 1301) to about half of the bottle volume, and the bottle is then pressurized with nitrogen to a specified equilibrium pressure (typically $\approx$ 4.1 MPa) at room temperature. The purpose of using the pressurization gas is to expedite the discharge of the agent and to facilitate the dispersion of the agent. Without nitrogen pressurization, the bottle pressure, which is simply the vapor pressure of the agent, can be so low at cold ambience that there is not enough driving force to rapidly expel the agent from the bottle when needed.

Present military specification (MIL-E-22285) [1] for CF_3Br in engine nacelle applications calls for a discharge time of less than 0.5 s and an amount of agent corresponding to a dwell time of 0.5 s throughout the protected nacelle space with an agent volume fraction of at least 0.06 at normal cruising condition. The certification process for the fire suppression system requires the use of a Halonyzer, a Federal Aviation Administration certified instrument, with 12 measurement probes positioned throughout the protected space to monitor the temporal CF_3Br concentration upon the discharge of the agent.

Due to its adverse effect on the ozone layer, halon 1301 has been banned from production in the United States since 1994 in compliance with the Montréal Protocol On Substances That Deplete The Ozone Layer. Many studies have since been conducted to identify alternatives to replace halon 1301. Trifluoroiodomethane (CF_3I) has been proposed as a potential replacement for

halon 1301 in aircraft engine nacelle fire protection applications [2,3]. One important aspect pertinent to CF_3I applications in an engine nacelle is the discharge behavior of the agent when it is exposed to ambient temperatures well below its normal boiling point. Such a condition may be encountered during a cold start of an engine on a cold tarmac or high-altitude cruising.

Table 1 lists some of the physical properties of CF_3I. For comparison and reference, the properties of CF_3Br are also given in the table. Since CF_3I has a normal boiling point of –22 ºC, the dispersion of CF_3I into air at temperatures down to –40 °C may not be as effective as halon 1301, which has a normal boiling point of –57.8 ºC.

Table 1. Selected physical properties of CF_3I and CF_3Br [4].

Agent	Molecular weight (kg/mol)	T_b (ºC)	T_c (ºC)	P_c (MPa)	ρ_c (kg/m^3)	P_s @ –40 ºC (kPa)	ΔH_v (kJ/kg)
CF_3I	0.196	–22.0	122.0	4.04	871	44.77[*]	106
CF_3Br	0.149	–57.8	67.0	4.02	745	224.4[§]	111

T_b is the normal boiling point; T_c is the critical temperature; P_c is the critical pressure; ρ_c is the critical density; P_s is the vapor pressure, ΔH_v is the latent heat of vaporization at T_b.
[*] from [5]
[§] from [6]

The release of CF_3I (at room temperature or chilled to about –40 °C) into a fire compartment and an engine nacelle simulator at ambient room temperature has been examined [4,7]; however, the discharge of cold CF_3I into a cold ambience has not been performed, or at least has not been documented in open literature. To the best of our knowledge, there is only one corporate internal report [8], which describes a study of the release of cold CF_3I into a well-mixed cold *enclosure* with *no* airflow. Careful examination of the data indicated some deterioration in the distribution of CF_3I within the enclosure when compared to room temperature conditions. In order to assure that there is no substantial deterioration in dispersion performance of CF_3I under cold temperature applications, discharge tests in an aircraft engine nacelle with airflow at –40 °C are needed. The temperature of –40 °C was selected in this study because it was below the normal boiling point of CF_3I and was the lowest operating temperature for some of the equipment used in the experiments.

At the HOTWC 2001 workshop [9], we presented some experimental data based on a series of discharge tests using CF_3I in a simulated aircraft engine nacelle with CF_3I (initially pressurized with nitrogen to ≈ 4.1 MPa at room temperature) at either –40 ºC or room temperature and airflow at room temperature. Since then, we have modified the nacelle simulator to better mimic the geometry and the flow characteristics inside a real nacelle. Using the *modified* simulator, we have performed CF_3I discharge tests at –40 ˚C with airflow through the nacelle at –40 ºC. This paper reports some of the data obtained from these tests.

APPARATUS

The experimental apparatus consisted of a simulated engine nacelle with baffles, an agent release port, four observation windows, and two measurement ports. Figure 1 is a schematic of the

simulator. The annulus of the simulator had an inside diameter of 0.6 m and an outside diameter of 0.9 m, resulting in a cross-sectional area of 0.35 m^2. The length (2 m) of the simulator was comparable to the distance between the agent injection port and the downstream end of a typical small engine nacelle. The baffle height was 0.075 m. The baffles were used to mimic a complicated flow path for the agent transport as in the case of a real nacelle. To modify the existing simulator [9], two baffles were added to the inner surface of the outer cylinder, and two longitudinal ribs with the same height as the baffles were placed on the outer surface of the inner core of the nacelle between the inner forward and aft baffles (see Figure 1). The ribs were used as barriers to prevent the agent from flowing circumferentially. The simulator was fabricated of 3.2 mm thick stainless-steel sheet metal.

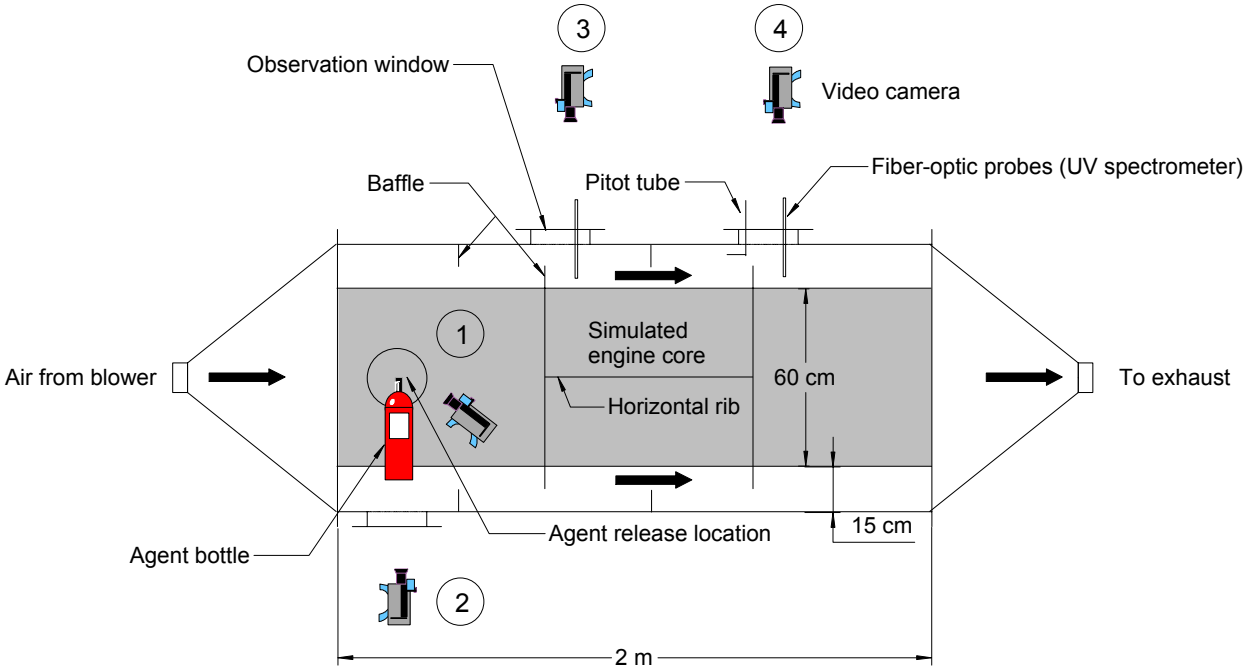

Figure 1. Schematic of the simulated engine nacelle.

A receiver bottle (Pacific Scientific[1], P/N 36200122) with an internal volume of 2.36 L was used to store CF_3I for discharge. A fast-response static pressure transducer (uncertainty ± 10 kPa) was mounted on the receiver bottle to monitor the pressure inside the bottle during filling and discharge. A K-type thermocouple (uncertainty ± 1 °C) was inserted into the bottle to record the temperature of the liquid agent before discharge. The agent was released using a quick-acting solenoid valve (Pacific Scientific, P/N 36400036). To tailor the agent discharge time (< 0.5 s), a reducer was placed at the valve exit. The agent was released through a vertical tee at the end of a short stainless-steel tubing (i.d. = 15.9 mm, o.d. = 19.1 mm) connected to the reducer.

Four CCD cameras (30 frames/s) were used to observe the agent discharge behavior at the release port (Camera 1), at a location in the bottom of the simulator to observe any pooling of

[1] Certain commercial products are identified in this paper in order to specify adequately the equipment used. Such identification does not imply recommendation by the National Institute of Standards and Technology, nor does it imply the equipment is the best available for the purpose.

agent (Camera 2), and at the two concentration measurement locations (Cameras 3 and 4), respectively. A frequency-controlled, variable-speed blower provided airflow through the nacelle simulator. The maximum air speed in the annulus, measured using a pitot tube, can reach 9.2 m/s at room temperature.

To achieve an operating temperature of –40 °C, the entire facility was housed inside the U.S. Army environmental test chamber at Ft. Belvoir, and the cold discharge experiments were conducted inside the chamber. The chamber has an interior dimension of 2.74 m (H) × 3.35 m (W) × 3.66 m (L) and a 1.83 m × 1.83 m sliding door. The lowest temperature attainable in the environmental test chamber is –54 °C. Discharge experiments at room temperature were also conducted inside the chamber without running the refrigeration unit to establish baselines for comparisons.

The experimental procedure involved the following steps. The receiver bottle was first filled with the required amount of agent and then pressurized with nitrogen to ≈ 4.1 MPa at room temperature. The bottle was connected to the discharge plumbing of the simulator and was ready for a discharge experiment. For cold temperature conditions, the environmental test chamber and the receiver bottle were cooled down to –40 °C before a test was commenced. Two contact K-type thermocouples were attached on the front and aft of the simulator external skin to monitor the ambient temperature of the chamber. In addition, a bare-beaded K-type thermocouple was placed in the annulus to measure the air temperature through the nacelle.

Based on the simulated nacelle volume and airflow, the amount of agent required for a fixed injection period (< 0.5 s for typical nacelle applications) was estimated using the generic nacelle modeling results discussed in Hamins *et al*. [10]. The agent bottle was charged with ≈ 1 kg of CF_3I and then pressurized with nitrogen to the desired pressure (≈ 4.1 MPa) at room temperature. Table 2 lists the experimental matrix. The airflow through the simulator was maintained at 1.5 kg/s ± 0.1 kg/s (mean ± standard deviation).

Table 2 Experimental matrix.

Nominal initial conditions of vessel	Nominal conditions of vessel before discharge	Nominal conditions in the simulator
22 ºC and 4.12 MPa	–40 ºC at prevailing P[§]	–40 ºC [§]
22 ºC and 4.12 MPa	22 ºC and 4.12 MPa	22 ºC (baseline)
22 ºC and 4.12 MPa	–40 ºC at prevailing P*	22 ºC

[§] Tests were performed in the environmental test chamber.

* Dry ice was used to cool the vessel.

The dispersion effectiveness of CF_3I was assessed based upon concentration measurements at the two locations inside the engine nacelle simulator (see Figure 1). Note that the intent of this work is not to address the certification process, which requires twelve measurement locations. The measurements were made using two Ocean Optics S2000 UV/VIS fiber-optic spectrometers. The optical components consisted of a deuterium/tungsten source, four (UV grade quartz) collimating lenses, and 300 μm diameter optical fibers. These were arranged to provide two

measurement locations (coincident with Cameras 3 and 4) approximately 0.75 m apart along the direction of the airflow in the engine nacelle testing apparatus. A bifurcated fiber (1 m in length, coupled with a 5 m extension) was used to connect the source to a pair of collimating lenses secured by brackets to the Plexiglas® viewing windows located on the top of the apparatus. The source radiation emanating from each lens was transmitted over a 0.038 m optical path (perpendicular to the airflow) to an opposing set of collimating lenses connected by independent optical fibers (5 m in length) to the master and slave spectrometers. Although the specifications indicated that these optical components should have a spectral range from 200 nm to 850 nm, very little throughput at wavelengths shorter than 250 nm was found.

The two spectrometers were software triggered by an electronic timer. The integration time (analogous to the shutter speed) was set at 30 ms, and the pixel resolution of the analogue to digital converter (ADC) was set at 10, which amounts to a spectral resolution of only about 3 nm. With this configuration, we were able to achieve a data acquisition rate of approximately 12 single scan spectra (6 at each location) per second to capture the time dependent details of the agent discharge.

An electronic timer was used to coordinate the experimental sequence of events. At t = 0 s, a signal was sent from the timer to trigger the data acquisition system to record the pressure of the discharge bottle and the pitot tube output at a sampling rate of 200 Hz. At t = 1 s, the timer initiated the two UV spectrometers, and at t = 2 s, the solenoid valve was activated to discharge the CF_3I/nitrogen mixture from the bottle into the engine nacelle simulator.

RESULTS AND DISCUSSION

The observations from Camera 1 showed that the agent discharge time at –40 ºC was longer than that at room temperature. When CF_3I was discharged at room temperature with airflow at the same temperature, the observations obtained from Camera 2 showed that a small amount of CF_3I pooled in the bottom of the simulator upon release. However, the liquid CF_3I boiled off within 66 ms. On the contrary, when CF_3I was discharged at –40 ºC with airflow at –40 ºC, a significant amount of liquid CF_3I pooled at the bottom of the nacelle upon release. The liquid CF_3I evaporated slowly and remained for many seconds (> 60 s) before complete evaporation. Intermediate behavior was observed when CF_3I was discharged at –40 ºC with airflow at room temperature. The observations from Cameras 3 and 4 showed that a cloud of CF_3I passed through the field of view of the cameras after agent discharge. The observations from Cameras 3 and 4 were qualitatively similar for the discharge of CF_3I at room temperature and –40 °C, irrespective of the temperature of the airflow.

The differences in pooling tendency described above can be explained in part due to the resulting high liquid fraction when the agent/nitrogen mixture is released at –40 ºC [4]. In addition, if the nacelle surface is at –40 ºC, the evaporation of the liquid pool will be very slow. The combined effects of pooling and slow evaporation will have an adverse impact on the subsequent dispersion of the agent/nitrogen mixture in the nacelle at –40 ºC.

The UV spectrometer was calibrated at 295 K using a quartz cell with an optical path length of 0.075 m. The cell was first evacuated to 1.33 Pa. Then, a fixed amount of CF_3I vapor was

metered into the cell by monitoring the cell pressure. Spectra were taken using an integration time of 30 ms and a pixel resolution of 10. Figure 2 shows a typical CF_3I absorption spectrum. Note that the peak absorbance for CF_3I centers around 270 nm. Although full CF_3I spectra were obtained in each test, a common practice used in spectroscopy to obtain the concentration measurements from the spectra is based on the wavelengths at the peak absorbance or its vicinity. The spectrometer is also equipped to take absorbance measurements at three specified wavelengths in addition to the full spectra. The wavelengths selected were 280 nm, 300 nm, and 500 nm. The absorbance at 300 nm was used to obtain the CF_3I concentration because saturation of the detector in the spectrometer at ≈ 280 nm was observed in some cases. The measurements at 500 nm (off-resonance) were used to indicate the presence or absence of liquid CF_3I droplets in the flow (see discussion below).

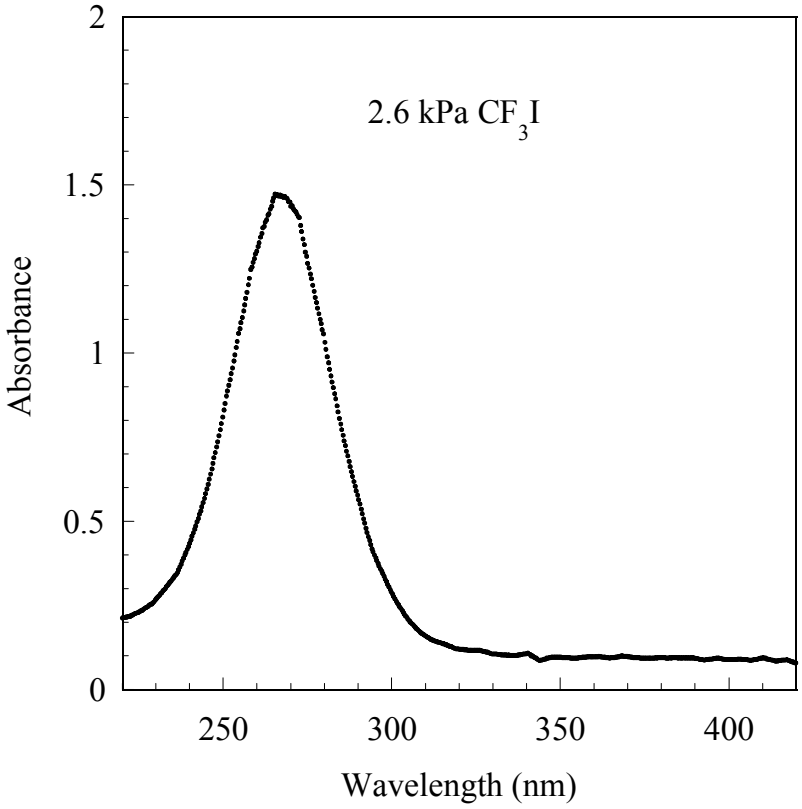

Figure 2. A typical CF_3I absorption spectrum.

The calibration curve (at λ = 300 nm and 295 K), which is a plot of absorbance (A) against concentration (C, molecules cm^{-3}), is shown in Figure 3.

According to the Bouguer-Beer-Lambert law,

$$A(\lambda) = -\log\left[\frac{I(\lambda)}{I_o(\lambda)}\right] = \frac{C\sigma(\lambda,T)L}{2.303} \quad (1)$$

where $I(\lambda)$ and $I_o(\lambda)$ are the incident and transmitted intensities through the cell respectively, $\sigma(\lambda, T)$ is the absorption cross section (cm^2), L is the optical path length (cm), T is the temperature, and λ is the wavelength. Note that the absorption cross section is a function of wavelength and temperature. Using the ideal gas law, Equation (2) gives the relationship between C and the partial pressure p (Pa) at 295 K.

$$C = 2.44\times10^{14}\, p \qquad (2)$$

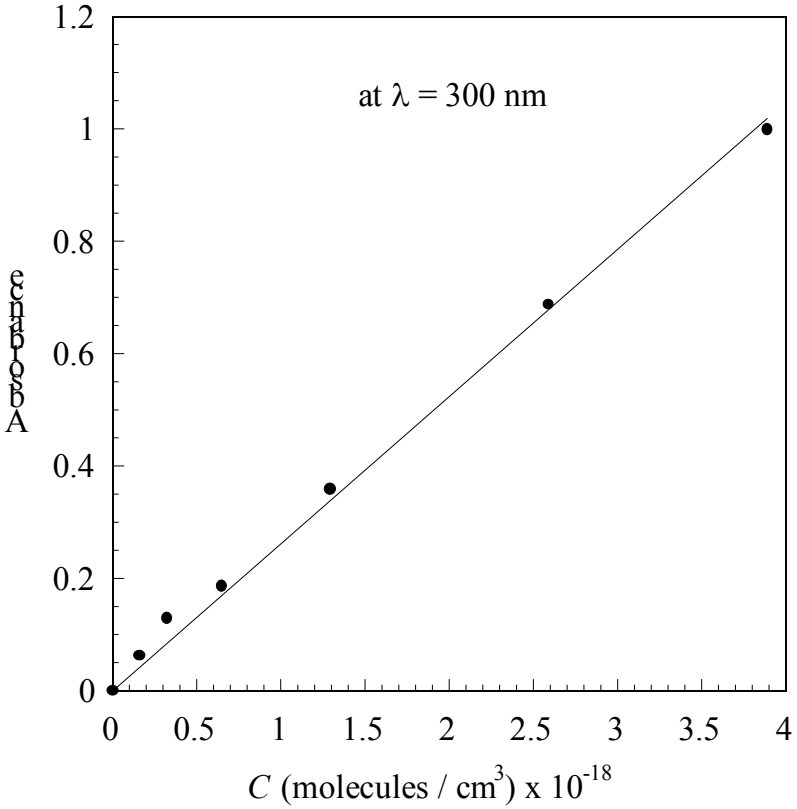

Figure 3. Calibration curve.

From Equation (1), the absorption cross section can be obtained from the slope of the calibration curve. A linear regression line is fitted through the data points in Figure 3, and the absorption cross section of CF_3I is 8.1×10^{-20} cm^2, which is comparable to the value of 8.9×10^{-20} cm^2 at λ = 300 nm and 295 K to 300 K in the literature [11]. Since the calibration was performed at 295 K, a correction for the temperature effect on the absorption cross section is necessary to obtain the CF_3I partial pressure at other prevailing temperatures, using the following equation [11]:

$$\sigma(\lambda, T) = \sigma(\lambda, 298\ \mathrm{K})\exp\left[B(\lambda)(T-298)\right] \qquad 210\ \mathrm{K} < T < 300\ \mathrm{K} \qquad (3)$$

The concentration C of CF_3I at any temperature was calculated from the absorbance measurement using Equations (1) and (3). At 300 nm, $B = 4.876\times10^{-3}$ K^{-1} [11]. The partial pressure of CF_3I was then obtained using the ideal gas law at the *prevailing* temperature.

However, the temperature effect on the absorption cross section was found to be negligible in the concentration calculations.

An estimate of the uncertainty (one standard deviation) of our measurements was obtained by comparing results at these settings to more accurate values obtained after signal averaging 100 scans at the full resolution of the spectrometer (≈ 0.3 nm). Based on this analysis, the CF_3I partial pressures reported in this paper are accurate to ± 15 %.

The concentration of CF_3I obtained at 300 nm is shown for both the room and cold temperature releases in Figures 4 and 5 for the two measurement locations, respectively. The initial time (t = 0) in the figures corresponds to the initiation of the agent release. Although three runs were performed at each condition with similar observations, only a single run for each condition is shown in the figure for clarity. The arrival times of the agent at the two measurement locations were clearly captured in the figures. Some salient features are noted in the two figures.

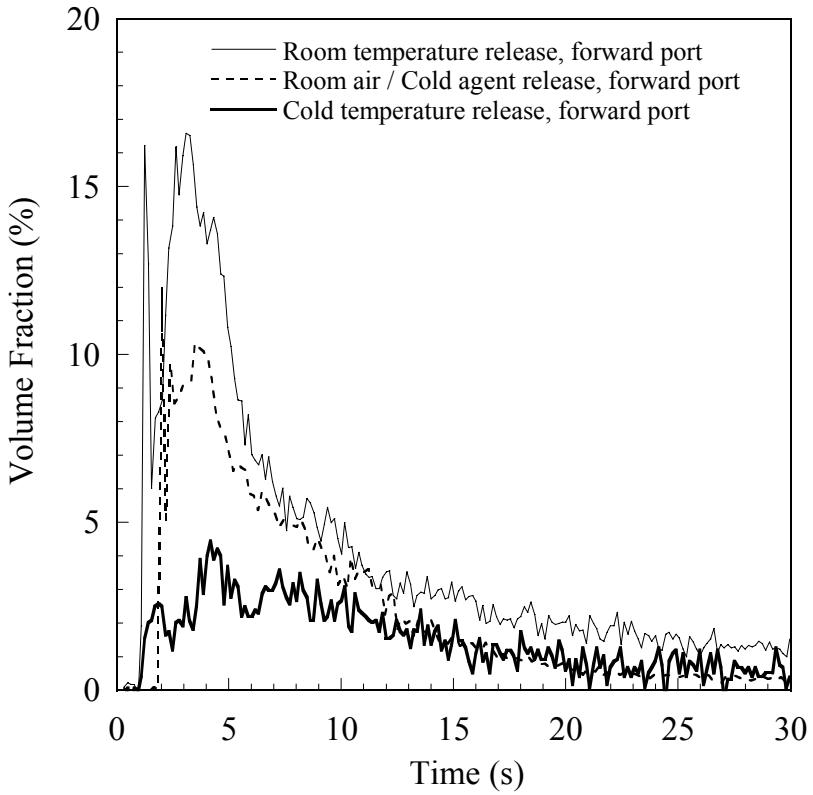

Figure 4. Concentration profiles of CF_3I at the forward measurement location under three test conditions.

For the room temperature release (both agent and air at room temperature), an initial spike was observed at the forward measurement location. This was due to the presence of a two-phase (liquid droplet-laden) flow because the off-resonance spectral measurement at 500 nm also showed a peak at the same time. The two-phase flow was the result of break-up of the liquid core into droplets at the discharge port. The off-resonance extinction at 500 nm indicated that

liquid CF_3I droplets were present for only a short period of time (< 2 s) immediately following the discharge. Therefore, it can be argued that the concentration measured after the initial spike in Figure 4 was due largely to the CF_3I vapor with minimal contribution from the droplets. The off-resonance spectral measurement at 500 nm in the aft location indicated that no droplets were present. The absence of the droplets and the much lower CF_3I concentration (see Figure 5) at this location indicated that the current nacelle simulator had indeed created a very challenging environment for agent dispersion, a condition which is generally true for a real engine nacelle. Furthermore, the generic nacelle model [10] provided a reasonable estimate of the amount of agent needed to achieve the required extinguishing concentration in the current nacelle. Halon 1301 and CF_3I have similar heptane cup-burner extinguishing concentration, a volume fraction of 0.032 [2]. Assuming that the military specification for halon 1301 can be applied to CF_3I, the measurements in Figures 4 and 5 suggest that a volume fraction of 0.06 can be attained over a duration of 0.5 s in both locations at room temperature. Based on the above reasoning, the current nacelle simulator mimics some of the operational features of a real nacelle.

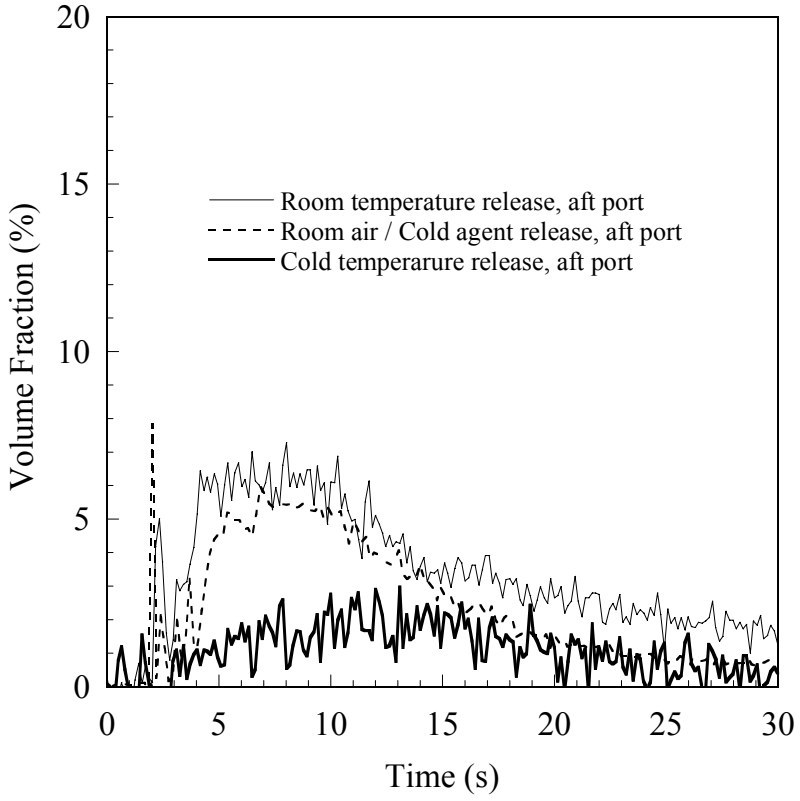

Figure 5. Concentration profiles of CF_3I at the aft measurement location under three test conditions.

For cold temperature release (both agent and air at –40 ºC), the off-resonance spectral measurements at 500 nm did not indicate the initial presence of droplets at both forward and aft measurement locations. The absence of the droplets was due partly to the reduction in the initial bottle pressure (≈ 3 MPa –40 ºC *vs*. ≈ 4.1 MPa at room temperature), which would impart less momentum to the droplets upon the release of the agent. Droplets with less momentum were less

likely to be transported to the two measurement locations. The combined effect of low bottle pressure and large liquid fraction in cold temperature release might generate larger droplets as a result of poor atomization of the liquid core, thus hindering the droplets from following the airflow. Similar to the room temperature release, the concentration at the forward location was higher than that at the aft. However, the difference was not as significant as in the case of room temperature release. The most important finding from this study was that there was a significant reduction in the agent concentration in the cold temperature release. At the forward measurement location, a reduction of a factor of almost 3 was observed at the peak concentration. At both locations, the agent concentration measurements were always *below* a volume fraction of 0.06.

Another set of experiments has also been carried out using agent at –40 ºC and airflow at room temperature. The results are also shown in Figures 4 and 5. An initial spike was again observed at the forward measurement location, an indication of the presence of droplets. The concentration distributions under these conditions are intermediate between the room and cold temperature releases. The room temperature airflow improves the dispersion and evaporation of the cold agent to a certain extent.

CONCLUSIONS

Discharge tests have been conducted at –40 ºC in an aircraft engine nacelle simulator placed inside an environmental test chamber. The temperatures of the airflow and the agent were found to have a significant effect on the subsequent dispersion of the agent upon its release. Comparing to the observations from room temperature discharge tests, the results at –40 ºC from the two measurement locations in the nacelle have shown that the dispersion of CF_3I under this condition is not very effective and there is substantial deterioration in agent concentration. If the required agent extinguishing concentration for the engine nacelle is based on room temperature test data, the effect of using the agent at a temperature much lower than its normal boiling point must be accounted for.

ACKNOWLEDGEMENTS

This research is part of the Department of Defense's Next Generation Fire Suppression Technology Program (NGP), funded by the DoD Strategic Environmental Research and Development Program (SERDP). Dr. Richard G. Gann of the National Institute of Standards and Technology (NIST) is the technical program manager. We would also like to thank Dr. Vladimir Orkin of the Chemical Sciences and Technology Laboratory (CSTL) of NIST for providing the calibration facility and his assistance in the calibration of the UV spectrometer and Dr. William L. Grosshandler of our laboratory for many stimulating discussions and encouragement. SLM also acknowledges the financial support from the National Research Council Postdoctoral Research Associateship.

REFERENCES

[1] Military Specification, MIL-E-22285 (Wep). *Extinguishing System, Fire, Aircraft, High-*

Rate-Discharge Type, Installation and Test of, 11 December 1959, Amendment – 1, 27 April 1960.

[2] Grosshandler W.L., Gann R.G., and Pitts W.M. (eds.), *Evaluation of Alternative in-Flight Fire Suppressants for Full-Scale Testing in Simulated Aircraft Engine Nacelles and Dry Bays*, NIST SP 861, April 1994, U.S. Department of Commerce, Washington, DC.

[3] Gann R.G. (ed), *Fire Suppression System Performance of Alternative Agents in Aircraft Engine and Dry Bay Laboratory Simulat*ions, Volumes. I and II, NIST SP 890, U.S. Department of Commerce, Washington, DC, November 1995.

[4] Yang, J.C., Cleary, T.G., Vazquez, I., Boyer, C.I., King, M.D., Breuel, B.D., Womeldorf, C.A., Grosshandler, W.L., Huber, M.L., Weber, L., and Gmurczyk, G., "Optimization of System Discharge," in Chapter 8, *Fire Suppression System Performance of Alternative Agents in Aircraft Engine and Dry Bay Laboratory Simulations*, Vol. I, Gann, R.G. (ed.), NIST SP 890, U.S. Department of Commerce, Washington, DC, November 1995.

[5] Smith, B.D. and Srivastava, R. *Thermodynamic Data for Pure Compounds, Part B, Halogenated Hydrocarbons and Alcohols*, Elsevier, Amsterdam, 1986.

[6] *NIST Thermodynamic Properties of Refrigerants and Refrigerant Mixtures Database (REPROP)*, V.4.0, NIST Standard Reference Data Program #23, NIST, Gaithersburg, MD, 1993.

[7] Guesto-Barnak, D., Sears, R., Simpson, T., "Engine nacelle fire protection using non-ozone depleting fire suppressants," *Proceedings of International Conference on Ozone Protection Technologies*, pp. 515-524, Washington, D.C., October 21-23, 1996.

[8] Meserve, W.J. Personal communication. Pacific Scientific, HTL/KIN-Tech Division, Document Number 51750579, Duarte, California, May 2000.

[9] Yang, J.C., Nyden M.R., and Manzello, S.L., "Cold Discharge of CF3I in a Simulated Aircraft Engine Nacelle," *Proceedings of Halon Options Technical Working Conference*, Albuquerque, New Mexico, 24-26 April 2001.

[10] Hamins, A, Cleary, TG, Borthwick, P, Gorchkov, N, McGrattan, K, Forney, G, Grosshandler, WL, Presser, C, and Melton, L., "Suppression of Engine Nacelle Fires," in Chapter 9, *Fire Suppression System Performance of Alternative Agents in Aircraft Engine and Dry Bay Laboratory Simulations*, Vol. II, Gann, R.G. (ed.), NIST SP 890, U.S. Department of Commerce, Washington, DC, November 1995.

[11] DeMore, W.B., Sander, S.P., Golden, D.M., Hampson, R.F., Kurylo, M.J., Howard, C.J., Ravishankara, A.R., Kolb, C.E., Molina M.J., "Chemical Kinetics and Photochemical Data for Use in Stratospheric Modeling, Evaluation Number 12," JPL Publication 97-4, January 15, 1997, Jet Propulsion Laboratory, California Institute of Technology, Pasadena, California.